

ORBITAL DEPENDENCE OF GALAXY PROPERTIES IN SATELLITE SYSTEMS OF GALAXIES

HO SEONG HWANG^{1,2} AND CHANGBOM PARK¹

Last updated: November 15, 2018

ABSTRACT

We study the dependence of satellite galaxy properties on the distance to the host galaxy and the orbital motion (prograde and retrograde orbits) using the Sloan Digital Sky Survey (SDSS) data. From SDSS Data Release 7 we find 3515 isolated satellite systems of galaxies at $z < 0.03$ that contain 8904 satellite galaxies. Using this sample we construct a catalog of 635 satellites associated with 215 host galaxies whose spin directions are determined by our inspection of the SDSS color images and/or by spectroscopic observations in the literature. We divide satellite galaxies into prograde and retrograde orbit subsamples depending on their orbital motion respect to the spin direction of the host. We find that the number of galaxies in prograde orbit is nearly equal to that of retrograde orbit galaxies: the fraction of satellites in prograde orbit is $50 \pm 2\%$. The velocity distribution of satellites with respect to their hosts is found almost symmetric: the median bulk rotation of satellites is -1 ± 8 km s⁻¹. It is found that the radial distribution of early-type satellites in prograde orbit is strongly concentrated toward the host while that of retrograde ones shows much less concentration. We also find the orbital speed of late-type satellites in prograde orbit increases as the projected distance to the host (R) decreases while the speed decreases for those in retrograde orbit. At R less than 0.1 times the host virial radius ($R < 0.1r_{\text{vir,host}}$) the orbital speed decreases in both prograde and retrograde orbit cases. Prograde satellites are on average fainter than retrograde satellites for both early and late morphological types. The $u-r$ color becomes redder as R decreases for both prograde and retrograde orbit late-type satellites. The differences between prograde and retrograde orbit satellite galaxies may be attributed to their different origin or the different strength of physical processes that they have experienced through hydrodynamic interactions with their host galaxies.

Subject headings: galaxies: evolution – galaxies: formation – galaxies: general – galaxies: morphology
– galaxies: properties

1. INTRODUCTION

In the hierarchical picture of galaxy formation, massive galaxies are formed through merger and accretion. Satellite galaxies associated with massive host galaxies, memorize the history of their accretion and interaction with host galaxies. In addition, they are distributed out to a few virial radii of the host galaxy. Therefore, they are excellent probes of the dark matter halos surrounding the host galaxies.

A great deal of effort has been made to understand the spatial distribution of satellite galaxies around their host galaxies. The radial distribution of the observed satellites was found to be more concentrated than that of sub-halos around galaxy-sized halos in N-body simulations (Chen et al. 2006), but consistent with dark matter distribution (van den Bosch et al. 2005; Chen et al. 2006). The studies of color dependence on the radial distribution of satellites revealed that the radial distribution of red satellites is more centrally concentrated than that of blue satellites (Sales et al. 2007; Chen 2008). Similarly, the radial distribution of early morphological type satellites is more centrally concentrated than that of late-type satellites (Ann et al. 2008; Wang et al. 2010). The angular distribution of satellite galaxies is also an issue, which has been extensively addressed (e.g., Prada et al. 2003;

Sales & Lambas 2004, 2005; Ann et al. 2008; Bailin et al. 2008; Wang et al. 2009).

Another interesting issue is the kinematic properties of satellite galaxies. Satellite galaxies can be divided into two classes based on their orbital motion: those in prograde orbit that rotate around the host in the same direction as the rotation of the host, and those in retrograde orbit that rotate in the opposite direction. Several important questions have been raised for these two classes: (1) what the number ratio of galaxies in prograde orbit to those in retrograde orbit is; (2) what the amplitude of mean bulk rotation of satellites is; and (3) whether there is a difference in physical properties between them.

Zaritsky et al. (1993) searched for the satellites around late-type spiral galaxies with a luminosity similar to the Milky Way, and found 69 satellites around 45 host galaxies (~ 1.5 satellites per host). For 35 satellites whose orbital velocity directions were determined, they detected a small amount of rotation for the satellite systems, $\sim 29 \pm 21$ km s⁻¹, in the same sense as the rotation of hosts' disk. They also found that the number of satellites in prograde orbit is nearly equal to that in retrograde orbit. However, in NGC 5084, Carignan et al. (1997) detected nine satellite galaxies, and found a clear excess of satellites in retrograde orbit (eight in retrograde orbit and one in prograde orbit). Using the expanded catalog of 115 satellites around 69 host galaxies, Zaritsky et al. (1997) found that the number of galaxies in prograde orbit is almost the same as that of galaxies in retrograde orbit.

hoseong.hwang@cea.fr, cbp@kias.re.kr

¹ School of Physics, Korea Institute for Advanced Study, Seoul 130-722, Korea

² CEA Saclay/Service d'Astrophysique, F-91191 Gif-sur-Yvette, France

Recently, Azzaro et al. (2006) measured the direction of rotation for some host galaxies in the list of satellite systems of Prada et al. (2003), and secured 76 satellites associated with 43 host galaxies of which orbital directions were determined. With this sample, they found that the fraction of galaxies in prograde orbit (f_{pro}) is ~ 0.6 , which is slightly larger than the previous results ($f_{\text{pro}} \sim 0.52$ in Zaritsky et al. 1997), but is broadly consistent with those from their N -body simulation ($f_{\text{pro}} \sim 0.55 - 0.60$). In the catalog of satellite systems extracted from the Sloan Digital Sky Survey (SDSS; York et al. 2000) Data Release 6 (Bailin et al. 2008), Herbert-Fort et al. (2008) determined the direction of rotation of some host galaxies by spectroscopic observations. They obtained the data for 78 satellites associated with 63 hosts. Combining these data with those for the satellites in Zaritsky et al. (1997), they found that the fraction of galaxies in prograde orbit is still 0.53 ± 0.04 , and mean bulk rotation of satellites is $37 \pm 3 \text{ km s}^{-1}$, in the same sense as the rotation of hosts' disk. Interestingly, they found that the peculiar velocity distribution of satellites is not a single Gaussian, but is described as the sum of two Gaussians.

As summarized above, most studies focused on the first two issues, the fraction of galaxies in prograde orbit and the amplitude of mean bulk rotation of satellites. The difference in physical properties between them, which is very important to understand the formation of satellite systems, has not been explored much. Moreover, the direction of rotation of host galaxy that is essential to know the orbit of satellites, has been determined by the expensive spectroscopic observations.

In this paper, we determine the direction of rotation of host galaxies using the color images provided by the SDSS without conducting spectroscopic observations (see §2.3 for details), and present the results of a study on the dependence of various physical properties of satellite galaxies on their orbits (prograde and retrograde orbits). In this paper we mean by ‘satellites’ as the galaxies that are much fainter than their host galaxies that are isolated from other bright galaxies. Therefore, they are like the conventional satellites associated with the Milky Way or Andromeda, and are rather different from the ‘satellites’ used in the N -body simulations or group/cluster studies where all galaxies (or dark halos) other than the brightest one (or the most massive one) are called satellites. Section 2 describes the observational data used in this study. Orbital dependence of the physical parameters of satellites are given in §3. Discussion and summary are given in §4 and §5, respectively.

2. OBSERVATIONAL DATA SET

2.1. Physical Parameters of Galaxies

We use a spectroscopic sample of galaxies in the SDSS DR7 (Abazajian et al. 2009). The physical parameters of galaxies that we consider in this study are r -band absolute Petrosian magnitude (M_r), morphology, $(u - r)$ color, equivalent width of $H\alpha$ emission line [$W(H\alpha)$], color gradient in $(g - i)$ color, concentration index (c_{in}), internal velocity dispersion (σ), and Petrosian radius in i -band (R_{Pet}). Here we give a brief description of these parameters.

The r -band absolute magnitude M_r was computed us-

ing the formula,

$$M_r = m_r - 5\log_{10}[r(z)(1+z)] - K(z) + E(z), \quad (1)$$

where $r(z)$ is a comoving distance at redshift z , $K(z)$ is K -correction, and $E(z)$ is the luminosity evolution correction. We adopt a flat Λ CDM cosmology with density parameters $\Omega_\Lambda = 0.73$ and $\Omega_m = 0.27$. The rest-frame absolute magnitudes of individual galaxies are computed in fixed bandpasses, shifted to $z = 0.1$, using Galactic reddening correction (Schlegel et al. 1998) and K -corrections as described by Blanton et al. (2003). The evolution correction given by Tegmark et al. (2004), $E(z) = 1.6(z - 0.1)$, is also applied. The distance $r(z)$ has a unit of $h^{-1}\text{Mpc}$ and the corresponding $5\log h$ in M_r will be omitted in this paper.

We adopt the galaxy morphology information from the SDSS DR7 release of the Korea Institute for Advanced Study value-added galaxy catalog (KIAS-VAGC; Choi 2010, in prep.). In this catalog galaxies are divided into early (ellipticals and lenticulars) and late (spirals and irregulars) morphological types based on their locations in the $(u - r)$ color versus $(g - i)$ color gradient space and also in the i -band concentration index space (Park & Choi 2005). The resulting morphological classification has completeness and reliability reaching 90%. We perform an additional visual check of the color images of galaxies to correct misclassifications by the automated scheme. In this procedure we changed the types of the blended or merging galaxies, blue but elliptical-shaped galaxies, and dusty edge-on spirals.

The $^{0.1}(u - r)$ color was computed using the extinction and K -corrected model magnitude. The superscript 0.1 means the rest-frame magnitude K -corrected to the redshift of 0.1, and will subsequently be dropped. We adopt the values of $(g - i)$ color, concentration index (c_{in}), and Petrosian radius R_{Pet} computed for the galaxies in KIAS-VAGC (Choi 2010, in prep.). The $(g - i)$ color gradient was defined by the color difference between the region with $R_{\text{gal}} < 0.5R_{\text{Pet}}$ and the annulus with $0.5R_{\text{Pet}} < R_{\text{gal}} < R_{\text{Pet}}$, where R_{gal} is the galactocentric radius and R_{Pet} is the Petrosian radius estimated in the i -band image. To account for the effects of flattening or inclination of galaxies, elliptical annuli were used to calculate the parameters. The (inverse) concentration index is defined by R_{50}/R_{90} , where R_{50} and R_{90} are semi-major axis lengths of ellipses containing 50% and 90% of the Petrosian flux in the i -band image, respectively.

The velocity dispersion values of galaxies are adopted from the DR7 release of New York University (NYU) VAGC (Blanton et al. 2005) and values of $H\alpha$ equivalent width are taken from the DR7 release of Max-Planck-Institute for Astrophysics (MPA)/John Hopkins University (JHU) VAGC (Tremonti et al. 2004).

2.2. Satellite Systems of Isolated Galaxies

Finding isolated satellite systems consists of two steps: identifying isolated galaxies and finding satellites associated with the isolated galaxies. We consider all SDSS galaxies with redshifts less than 0.03 as the host candidates. Only the relatively nearby galaxies are considered because the visual determination of the sense of rotation is feasible only when the galaxy image shows detailed internal features. For each galaxy its neighbors are

searched. The neighbors of a target galaxy with a r -band absolute magnitude M_r are the galaxies with an absolute magnitude brighter than M_r+1 and a velocity difference less than Δv . We adopt $\Delta v = 1000 \text{ km s}^{-1}$ for early-type target galaxies, and 750 km s^{-1} for late-type galaxies based on the distributions of pairwise velocity difference of the SDSS galaxies (see Fig. 2 of Park & Choi 2009 and Fig. 1 of Wang et al. 2009). The neighbors are searched in the redshift interval from -0.005 to 0.034 . When a target galaxy has a projected distance to its neighbor galaxies (R_{nei}) larger than $\max[r_{\text{vir,target}}, r_{\text{vir,nei}}]$ for all neighbors, it is selected as an isolated galaxy. Here r_{vir} is the virial radius of a galaxy (see eq. (5) of Park & Choi 2009).

Once isolated host candidates are determined, the satellites associated with them are searched for. A galaxy qualifies as a satellite if it has an absolute magnitude fainter than $M_r(\text{host})+1$, velocity difference less than 600 km s^{-1} , and projected separation of the galaxy with the host $R < \min[R_{\text{nei}} r_{\text{vir,host}} / (r_{\text{vir,host}} + r_{\text{vir,nei}}), R_{\text{nei}} - r_{\text{vir,nei}}]$ where R_{nei} is a projected separation between the host and host's neighbor. The first limit divides the distance between the host and neighbor in proportion to their virial radii. The second limit prohibits the galaxies within the virial radii of the neighbor galaxies from being selected as satellites. In our SDSS galaxy sample we find 8904 satellites associated with 3515 isolated host galaxies.

2.3. Spin Direction of Host Galaxies

To determine the sense of rotation of host galaxies from their images we first assume that all spiral galaxies have trailing arms (Binney & Tremaine 1987) and determine the receding side of the major axis from their color images. The part of minor axis behind the bulge often appears smooth due to the foreground bulge stars while the side of the minor axis closer than the bulge often shows interstellar dust patches of relatively higher sharpness (Mihalas & Binney 1981). When it is not possible to determine the sense of rotation due to various reasons, we simply drop the host galaxy. Very early-type galaxies with smooth disks, very late-type galaxies with vanishing bulge, and nearly face-on or edge-on disk galaxies are difficult to assign the spin direction. After we remove all these cumbersome cases, we can determine the spin vector directions for 165 host galaxies that have 535 satellite galaxies.

We supplemented our sample by adding host galaxies of which rotation sense was determined from the spectroscopic observations in the literature (Rubin et al. 1982, 1985, 1999; Broeils & van Woerden 1994; Han et al. 1995; Taylor et al. 1995; Rhee & van Albada 1996; Zaritsky et al. 1997; Sofue 1997; Sofue et al. 1997, 1998, 2003; Héraudeau & Simien 1998; Héraudeau et al. 1999; Vega Beltrán et al. 2001; Garrido et al. 2002, 2003, 2004, 2005; Vogt et al. 2004; Coccato et al. 2004; Fridman et al. 2005; Hernandez et al. 2005; Noordermeer et al. 2005; Chemin et al. 2006; Falcón-Barroso et al. 2006; Daigle et al. 2006; Ganda et al. 2006; Azzaro et al. 2006; Herbert-Fort et al. 2008; Epinat et al. 2008a,b; Swaters et al. 2009). We compiled 390 satellites associated with 116 hosts. There are 51 hosts in common between the hosts of which rotation sense was deter-

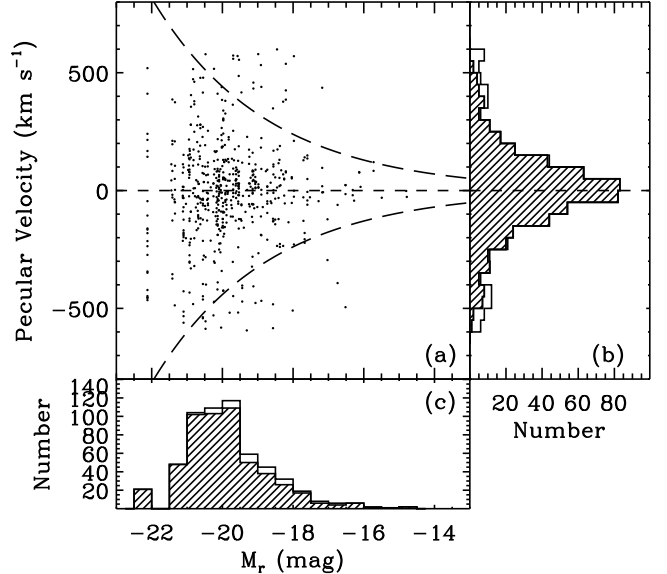


FIG. 1.— (a) Peculiar velocities of satellites as a function of absolute magnitudes of late-type host galaxies. Dashed-line envelopes indicate the velocity criteria for rejecting interlopers. (b) Distribution of absolute magnitudes of all hosts (open histogram) and of those having satellites within the velocity criteria (shaded histogram). (c) Distribution of peculiar velocities of all satellites (open histogram) and of those within the velocity criteria (shaded histogram).

mined in this study and those in the literature. We have compared our determination of the rotation sense with that in the literature for these common objects, and found that there is only one galaxy (NGC 5894) that shows a disagreement between the two. We kept the rotation sense for this object determined from the spectroscopic observation in the literature. In total, we have 727 satellites assigned to 230 hosts whose spin vector directions are known.

Among 727 satellites, we eliminated 45 spurious sources (e.g., faint fragments of bright galaxies, diffraction spikes of bright stars) that were included in the list of satellites (originally included in the spectroscopic sample of galaxies in SDSS) by inspecting color images of the satellites. In the result, 682 satellites with 221 host galaxies remain.

It is noted that our list contains some satellite systems whose host galaxies are early types because their spin directions were determined from the spectroscopic observations. Since the morphology of satellite galaxies is strongly affected by the morphology of host galaxies as found in Ann et al. (2008), we further divide the satellites into two categories (the cases of early- and late-type hosts) and obtain 197 late-type host galaxies having 579 satellite galaxies and 24 early-type hosts with 103 satellites. Our analysis will be restricted to the satellite systems with late-type hosts except §4.1.

In Figure 1, we plot peculiar velocities of satellite galaxies as a function of absolute magnitudes of host galaxies. The peculiar velocity of a satellite is defined by, $v_{\text{pec}} = S(v_{\text{sat}} - v_{\text{host}})$, where v_{sat} and v_{host} are observed velocities of the satellite and the host, respectively. S is defined by

$$S = \begin{cases} +1, & \theta < 90^\circ, \\ -1, & \text{otherwise.} \end{cases}$$

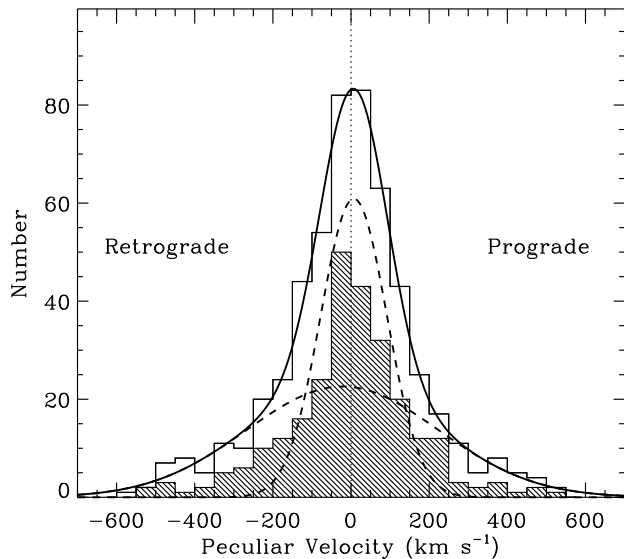


FIG. 2.— Peculiar velocity distribution for all satellite galaxies associated with late-type host galaxies. The vertical dotted line indicates zero velocity. Dashed lines represent the double Gaussian fits, and the solid line indicates the sum of two Gaussian functions. The hatched histogram indicates the peculiar velocity distribution of satellite galaxies located near the major axis of the hosts ($\theta < 45^\circ$).

$\theta = |\text{PAred} - \text{PAS}|$ where PAred is a position angle of the receding side of the host’s major axis, and PAS is the position angle of the satellite with respect to the host. All position angles are measured from north to east. Therefore, the satellites with $v_{\text{pec}} > 0$ rotate around the host in the same direction as the rotation of the host (prograde orbit) and those with $v_{\text{pec}} < 0$ rotate in the opposite direction (retrograde orbit).

Since the probability for a galaxy to become a satellite of a host decreases as the mass (luminosity) of the host decreases, we exclude some probable interlopers located outside the region bounded by dashed lines in Figure 1. The dashed lines are determined as follows. The escape velocity of a satellite can be given by $v_{\text{esc}} \propto (M_{\text{host}}/R)^{0.5}$ where M_{host} is a mass of the host and R is a projected distance to the host. The mass of the host galaxy is computed by $M_{\text{host}} = \gamma L$ where γ is the mass-to-light ratio and L is the r -band luminosity of the host. We assume that $\gamma(\text{early}) = 2\gamma(\text{late})$ at the same r -band luminosity, and that γ is constant with galaxy luminosity for a given morphological type (Park et al. 2008). Then we obtain $v_{\text{esc}}(M_r) = v_0 10^{(-0.4/3)(M_r - M_0)}$ in a given distance to the host galaxy (e.g., $R = r_{\text{vir,host}}$). We adopt $v_0 = 600 \text{ km s}^{-1}$ and $M_0 = -21 \text{ mag}$, and plot v_{esc} versus M_r as dashed lines in Figure 1.

The virial radius of a host galaxy ($r_{\text{vir,host}}$) is defined by the projected radius where the mean mass density ρ within the sphere of radius r is 200 times the critical density or 740 times the mean density of the universe, namely,

$$r_{\text{vir}} = (3\gamma L / 4\pi / 200\rho_c)^{1/3}. \quad (2)$$

Since we adopt $\Omega_m = 0.27$, $200\rho_c = 200\bar{\rho} / \Omega_m = 740\bar{\rho}$ where $\bar{\rho}$ is the mean density of the universe. The value of mean density of the universe, $\bar{\rho} = (0.0223 \pm 0.0005)(\gamma L)_{-20} (h^{-1} \text{Mpc})^{-3}$, was adopted, where $(\gamma L)_{-20}$ is the mass of a late-type galaxy with

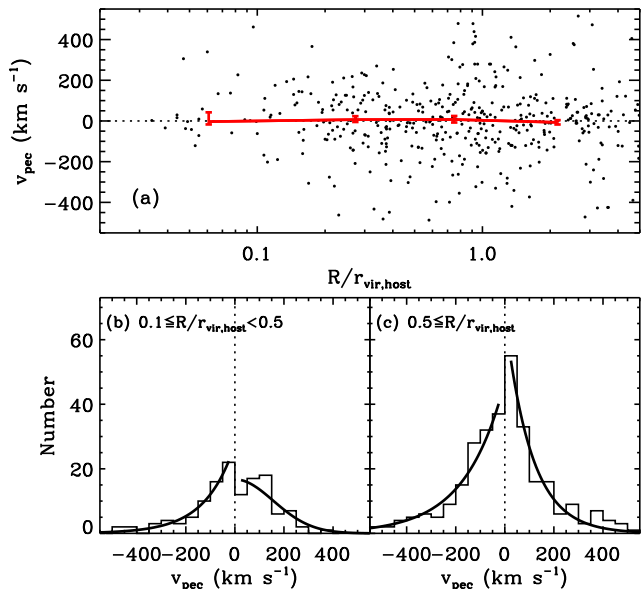


FIG. 3.— (a) Peculiar velocity v_{pec} vs. projected distance to the host galaxy. Median values in each radial bin and their errors are connected by solid lines. Peculiar velocity distribution for the satellites (b) at $0.1 \leq R/r_{\text{vir,host}} < 0.5$ and (c) at $0.5 \leq R/r_{\text{vir,host}}$. The vertical dotted lines indicate zero velocity. Solid lines indicate the best fit exponential functions of the distributions of satellites in prograde or retrograde orbits separately. Solid line for the satellites in prograde orbit at $0.1 \leq R/r_{\text{vir,host}} < 0.5$ is the best fit Gaussian function.

$M_r = -20$ (Park et al. 2008). According to our formula the virial radii of galaxies with $M_r = -19.5, -20.0,$ and -20.5 are 260, 300, and $350 h^{-1} \text{ kpc}$ for early types, and 210, 240, and $280 h^{-1} \text{ kpc}$ for late types, respectively. By rejecting probable interlopers as shown in Figure 1, we finally secured 534 satellite galaxies associated with 191 late-type hosts and 101 satellites associated with 24 early-type hosts.

We present the peculiar velocity distribution of all 534 satellite galaxies in Figure 2. The fraction of galaxies in prograde orbit (f_{pro}) is found to be $50 \pm 2\%$, and the median value of the peculiar velocity distribution is $-1 \pm 8 \text{ km s}^{-1}$. When we use only 262 satellites located near the major axis of the hosts ($\theta < 45^\circ$), f_{pro} does not change and the median value of the distribution is $0 \pm 10 \text{ km s}^{-1}$. We fit the peculiar velocity distribution using the sum of two Gaussian functions, and find the best-fit function with mean values of $\langle v_{\text{pec}} \rangle = 7 \text{ km s}^{-1} (\sigma = 85 \text{ km s}^{-1})$ and $\langle v_{\text{pec}} \rangle = -22 \text{ km s}^{-1} (\sigma = 246 \text{ km s}^{-1})$. When we fit the peculiar velocity distribution of satellites in prograde or retrograde orbits separately using a single Gaussian or exponential function, we find that the exponential function fits the distribution better than the Gaussian function. The reduced χ^2 for satellites in prograde orbit, are 2.1 and 0.5 for Gaussian and exponential functions, respectively. The reduced χ^2 for satellites in retrograde orbit are 2.5 and 0.7 for Gaussian and exponential functions, respectively.

To study whether or not the peculiar velocity distribution changes depending on the distance to the host we show the distribution for satellites at $0.1 \leq R/r_{\text{vir,host}} < 0.5$ or at $0.5 \leq R/r_{\text{vir,host}}$ separately in Figure 3. We use Gaussian and exponential functions to fit the distributions of satellites in prograde and retrograde orbits, and show best-fit functions in Figure 3(b-c). It is seen

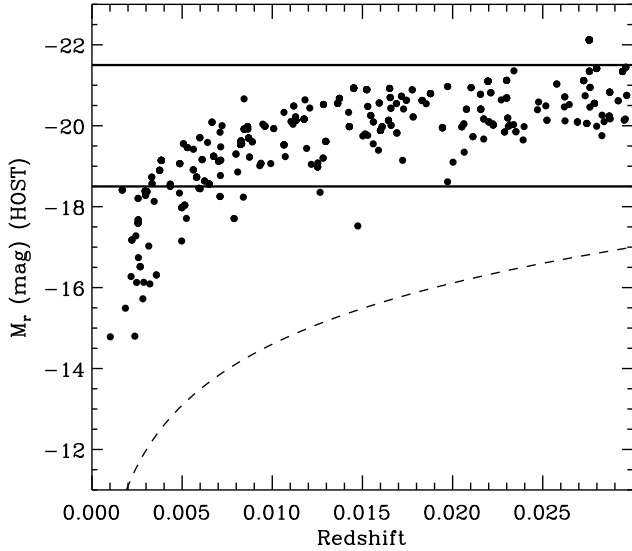


FIG. 4.— Absolute magnitude vs. redshift for late-type host galaxies. The dashed line is the apparent magnitude limit ($m_r = 17.77$) computed from eq. (1) in Choi et al. (2007). The satellites associated with the host galaxies within the solid box are selected as a luminosity subsample of satellites.

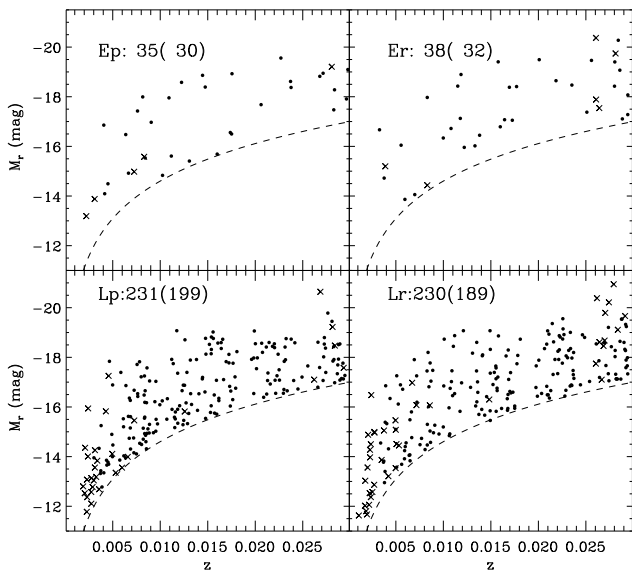


FIG. 5.— Absolute magnitude vs. redshift for early-type satellites in prograde orbit (Ep), for early-type satellites in retrograde orbit (Er), for late-type satellites in prograde orbit (Lp), and for late-type satellites in retrograde orbit (Lr). Satellites of the host galaxies in the luminosity subsample ($-18.5 \geq M_{r,\text{host}} > -21.5$) are filled circles, while the rests are crosses. Number outside the parenthesis means the number of galaxies in each panel, and the number in the parenthesis indicates the number of galaxies within the luminosity subsample.

that the best-fit function for satellites in retrograde orbit is exponential both in the inner and outer regions, while that for satellites in prograde orbit changes from Gaussian (inner region) to exponential (outer region).

We plot r -band absolute magnitudes of host galaxies and their satellites as a function of redshift in Figures 4 and 5. We made a luminosity subsample of satellites whose hosts have absolute magnitudes in the range of $-18.5 \geq M_r > -21.5$.

In Figure 6, we plot peculiar velocities of satellites as

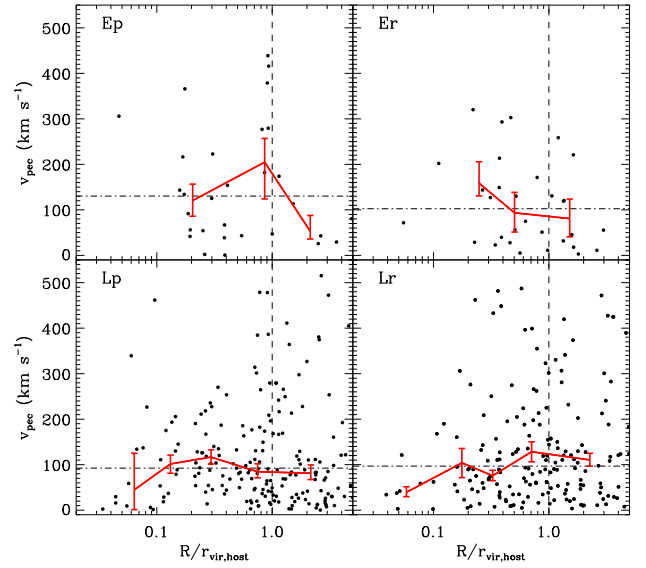


FIG. 6.— Peculiar velocity v_{pec} vs. projected distance to the host galaxy for early-type satellites in prograde orbit (Ep), for early-type satellites in retrograde orbit (Er), for late-type satellites in prograde orbit (Lp), and for late-type satellites in retrograde orbit (Lr) in the luminosity subsample. Global median values are shown by horizontal dot-dashed lines, and the median value in each radial bin is connected by the solid line. Vertical dashed line indicates one virial radius of the host.

a function of a distance to host galaxies. It shows that global median values of v_{pec} do not significantly vary depending on the orbit or morphology. However, there exists an interesting trend that v_{pec} of the late-type satellites in prograde orbit (Lp) increases as they approach the host, while v_{pec} of those in retrograde orbit (Lr) decreases. At the merger scales with $R/r_{\text{vir,host}} < 0.1$ the orbital velocity decreases for both Lp and Lr cases.

3. RESULTS

3.1. Spatial Distribution of Satellites

In Figure 7, we plot the radial distribution of satellites in prograde and retrograde orbits. We also show the fraction of galaxies in prograde orbit (f_{pro}) as a function of the projected distance to host galaxies. The top panel shows that satellites in prograde orbits are located closer to their hosts compared to those in retrograde orbits for the case of early-type satellites. However, we do not find such dependence of the spatial distribution of late-type satellites on their orbits (see panel c). As a result, f_{pro} of early types increases as R decreases, but f_{pro} of late types remains constant (~ 0.5) within the error bar.

To study whether or not satellites are concentrated on the plane of host galaxies' disk, we plot the ratio of the dispersion of satellite distribution along ($\sigma(\cos\theta)$) and perpendicular ($\sigma(\sin\theta)$) to the major axis of the host as a function of the ratio of minor axis to the major axis of the host ($(b/a)_{\text{HOST}}$) in Figure 8. It shows neither of the distributions of prograde or retrograde orbit satellites is aligned with late-type host galaxies.

3.2. Luminosity

Figure 9 shows absolute magnitudes of the satellites in the luminosity subsample as a function of the projected distance to host galaxies. Each panel represents different subsamples depending on morphology and orbit. For

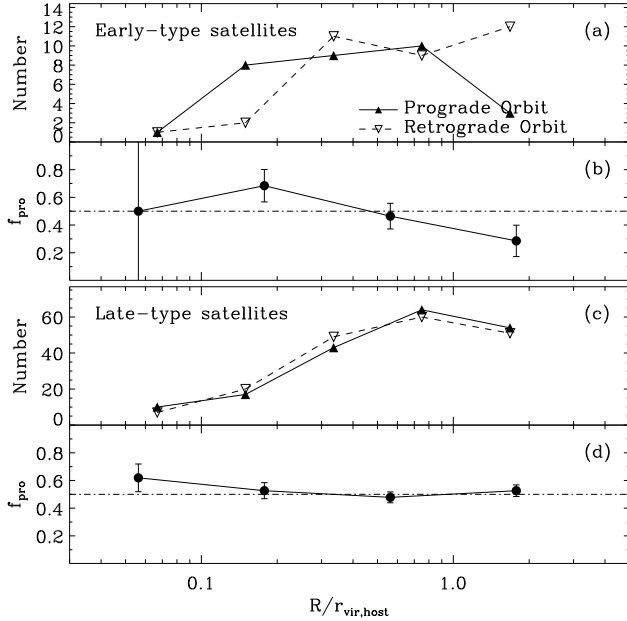


FIG. 7.— Distribution of early-type satellites in prograde (filled triangles) and retrograde (open upside-down triangles) orbits (a) and the number fraction of satellites in prograde orbit (f_{pro}) among early-type satellites (b) as a function of the projected distance to the host galaxies. Distribution of late-type satellites in prograde (filled triangles) and retrograde (open upside-down triangles) orbits (c) and f_{pro} among late-type satellites (d).

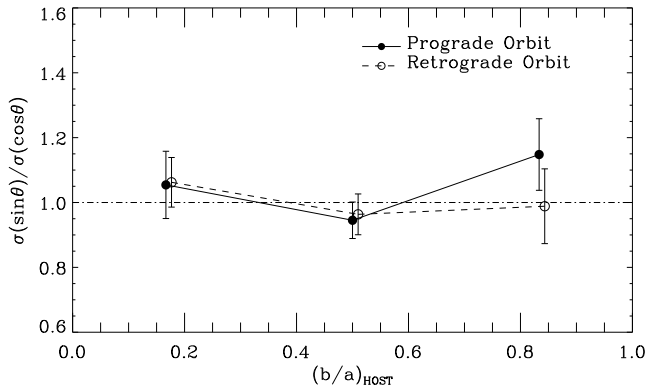


FIG. 8.— Ratio of the dispersions of satellite distribution along ($\sigma(\cos\theta)$) and perpendicular ($\sigma(\sin\theta)$) to the major axis of hosts as a function of the host axis ratio. Solid and dashed lines indicate satellites in prograde and retrograde orbits, respectively.

both early and late types, galaxies in retrograde orbit, on average, appear to be slightly brighter than those in prograde orbit. A statistical test with Monte Carlo simulation to compute the significance of the difference in the median of the physical quantity (to be discussed in the end of this section) confirms this difference for only late types with a significance level of 97%. When we compare satellites in each radial bin, the Monte Carlo test indicates with a significance level of 99% that median absolute magnitudes of late-type galaxies in the outer region ($R > r_{\text{vir,host}}$) are different depending on the orbit.

To investigate the difference in the galaxy luminosity depending on the orbit in more detail, we show the distribution of absolute magnitudes in Figure 10. We count the number of satellites within the redshift limit defined

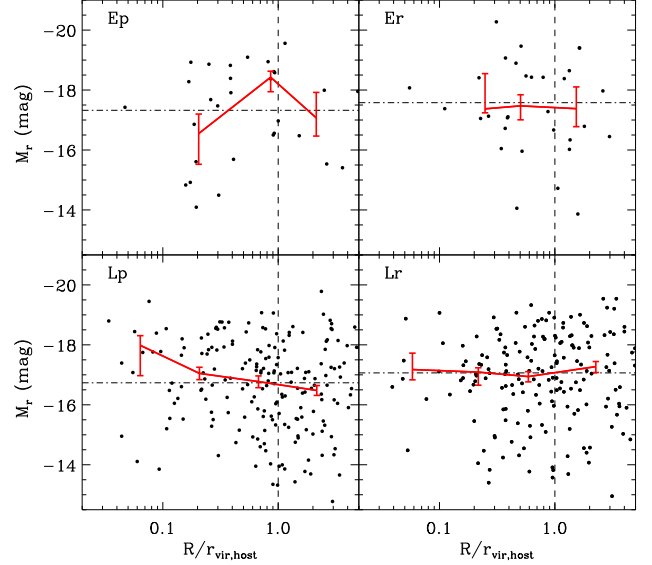


FIG. 9.— Same as Fig. 6, but for absolute magnitude M_r .

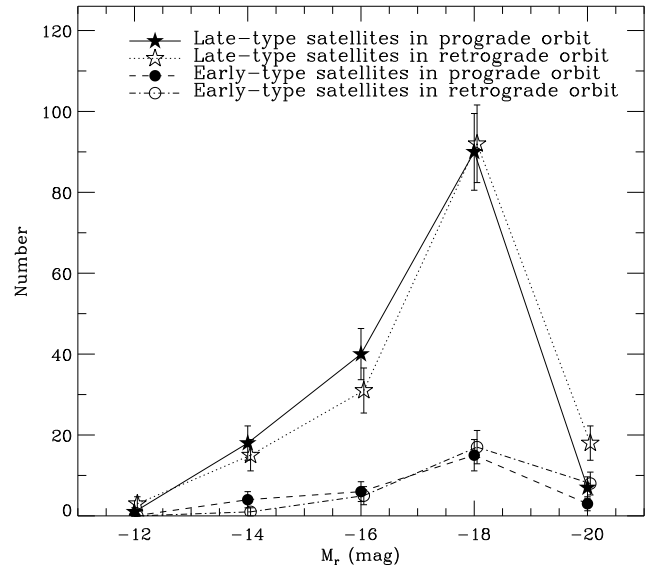
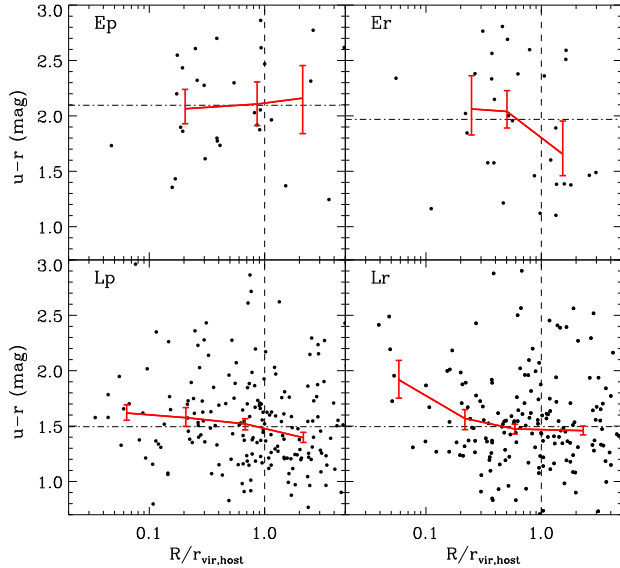


FIG. 10.— Distribution of absolute magnitudes for all satellite galaxies. Solid and dotted lines, respectively, indicate luminosity functions (LFs) for late-type satellites in prograde and retrograde orbits. Dashed and dot-dashed lines denote LFs for early-type satellites in prograde and retrograde orbits, respectively.

by the apparent magnitude limit in Figure 5, and do not correct the count for different volumes. It is seen that bright satellites ($-18 \geq M_r > -20$) in retrograde orbit are more numerous compared to those in prograde orbit. The test with Monte Carlo simulation confirms this result with a significance level of 97% in the sense that median absolute magnitudes of late types in prograde and retrograde orbits are significantly different.

We summarize the results of statistical comparison of several physical parameters between satellites in prograde and retrograde orbits and between satellites in the inner and outer regions in Tables 1 and 2, respectively.

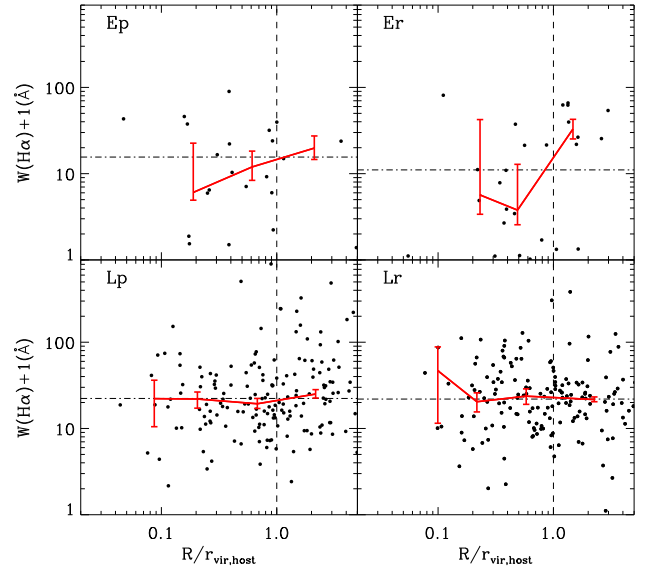
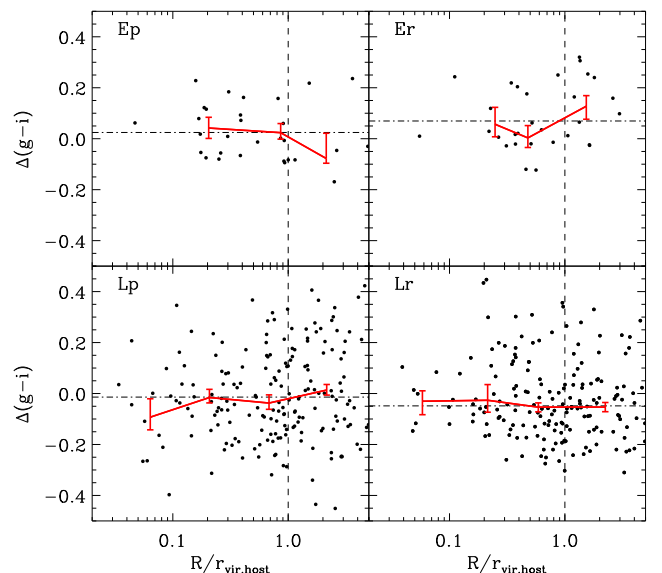
The statistical significance of the difference in the median or the dispersion of physical quantities, is computed

FIG. 11.— Same as Fig. 6, but for $(u - r)$ color.

by Monte Carlo simulations. For a given physical parameter, we construct two subsamples (with the same number of galaxies as in the actual prograde and retrograde samples) by randomly drawing the observed parameters from the whole early-type or late-type satellite galaxy sample and compute the median and the dispersion of each subsample. The resulting two subsamples will have the same medians and standard deviations on average. These random subsamples will tell us about whether or not the difference in the parameter between prograde and retrograde satellite samples is statistically significant. We construct 1000 trial data sets and compute the fraction of simulated data sets in which the difference of the physical quantity is larger than or equal to that based on the real data ($f_{\text{sim} \geq \text{obs}}$). The significance levels of the difference defined by $100(1 - f_{\text{sim} \geq \text{obs}})$ (%) are given in Tables. We have applied the statistical tests to all the physical parameters, but only show statistically significant results (significance level above 95%) in the Tables.

3.3. Star Formation Activity Parameters

Figure 11 shows $(u - r)$ colors of satellite galaxies divided by their morphologies and orbital motion as a function of the projected distance to the hosts. The late-type satellites in prograde and retrograde orbits have a similar global median value, and both show a hint of an increase in $(u - r)$ color with decreasing R . In the Monte Carlo test for the radial gradient we divide each sample into inner ($R < r_{\text{vir,host}}$) and outer ($R \geq r_{\text{vir,host}}$) regions, and test if the difference in the physical parameter in two regions is statistically significant. The random subsamples are generated in such a way that a parameter value is randomly drawn from the combined sample and assigned to a galaxy in inner or outer region. The resulting subsamples will have no radial gradient in the parameter and have the same dispersions on average. A test with such Monte Carlo simulation confirms that the change of $(u - r)$ color with R for late types in prograde orbit (see Tab. 2) is significant at a 99% confidence level. It is noted that the increase of $(u - r)$ colors for those

FIG. 12.— Same as Fig. 6, but for equivalent width of $H\alpha$ line.FIG. 13.— Same as Fig. 6, but for $(g - i)$ color gradient.

in retrograde orbit is very strong in the innermost region ($R < 0.1 r_{\text{vir,host}}$) even though the overall gradient is not significant.

In Figure 12, we plot the equivalent width of $H\alpha$ lines of satellite galaxies, which is a useful measure of star formation activity (SFA). For late-type satellites, the median values of $W(H\alpha)$ for two subsamples are similar, and those do not seem to change with R for both samples even though their $(u - r)$ colors become redder at smaller R as seen in Figure 11. However, the test with Monte Carlo simulation shows that the difference in the dispersion of $W(H\alpha)$ between late-type satellites in prograde and retrograde orbits is remarkable with a significance level of of 97% (see Tab. 1). The difference in the dispersion of $W(H\alpha)$ of retrograde orbit satellites in the inner and outer regions is also noted (see Tab. 2).

Figure 13 represents $(g - i)$ color gradients of satel-

TABLE 1
STATISTICAL COMPARISON BETWEEN SATELLITES IN PROGRADE AND RETROGRADE ORBITS

Parameter	Type	MC _{m,all}	MC _{d,all}	MC _{m,in}	MC _{d,in}	MC _{m,out}	MC _{d,out}	Remarks
(1)	(2)	(3)	(4)	(5)	(6)	(7)	(8)	(9)
M_r	L	97	58	49	40	99	69	Fig. 9
W(H α)	L	56	49	33	11	89	97	Fig. 12
$\Delta(g-i)$	L	95	98	66	72	98	98	Fig. 13
c_{in}	L	38	98	47	88	38	97	Fig. 14

Column descriptions. (1): Physical parameters. (2): Morphological types (E: early types, L: late types). (3): Significance level (%) of the difference of the median of the physical parameter between satellites in prograde and retrograde orbits determined from Monte Carlo simulation. (4): Significance level (%) of the difference of the dispersion of the physical parameter between satellites in prograde and retrograde orbits determined from Monte Carlo simulation. (5): Same as column (3), but for satellites in the inner region ($R < 1r_{vir,host}$). (6): Same as column (4), but for satellites in the inner region. (7): Same as column (3), but for satellites in the outer region ($R \geq 1r_{vir,host}$). (8): Same as column (4), but for satellites in the outer region ($R \geq 1r_{vir,host}$). (9): Relevant figure. Statistically significant values ($\geq 95\%$) are represented in bold face.

TABLE 2
STATISTICAL COMPARISON BETWEEN SATELLITES IN THE INNER AND OUTER REGIONS

Parameter	Type	MC _{m,pro}	MC _{d,pro}	MC _{m,ret}	MC _{d,ret}	Remarks
(1)	(2)	(3)	(4)	(5)	(6)	(7)
$(u-r)$	L	99	67	88	65	Fig. 11
W(H α)	L	13	12	64	97	Fig. 12
$\Delta(g-i)$	E	96	61	4	43	Fig. 13
R_{Pet}	E	97	77	90	24	Fig. 16
$(u-r)$	L	99	98	11	27	Fig. 17
$(u-r)$	L	93	98	90	67	Fig. 18

Column descriptions. (1): Physical parameters. (2): Morphological types (E: early types, L: late types). (3): Significance level (%) of the difference of the median of the physical parameter of prograde orbit satellites in the inner and outer regions determined from Monte Carlo simulation. (4): Significance level (%) of the difference of the dispersion of the physical parameter of prograde orbit satellites in the inner and outer regions determined from Monte Carlo simulation. (5): Same as column (3), but for retrograde orbit satellites. (6): Same as column (4), but for retrograde orbit satellites. (7): Relevant figure. Statistically significant values ($\geq 95\%$) are represented in bold face.

lite galaxies. The positive $(g-i)$ color gradient means a bluer color in the central region of a galaxy than that in the outer region. For early types, the difference of median $(g-i)$ color gradients of satellites in prograde orbit (Ep) between in the inner and outer regions is noticeable, which is supported by the test with Monte Carlo simulation (see Tab. 1). For late types, the test with Monte Carlo simulation suggests that the median and its dispersion of $(g-i)$ color gradients of satellites in prograde and retrograde orbits are different significantly in the whole/outer region.

3.4. Structure Parameters

Figure 14 shows the distribution of the concentration index c_{in} for satellite galaxies divided by their morphologies and orbital motion. Small value of c_{in} means that the light of a galaxy is more concentrated in the central region. It is found that the global median and the scatter of c_{in} values for early-type satellites are not significantly different depending on their orbits. However, it is noted that there are few early types in retrograde orbit with large c_{in} values (> 0.4) in the inner region ($R < 0.2r_{vir,host}$), and few early types in prograde orbit with large c_{in} values (> 0.4) are found in the outer region

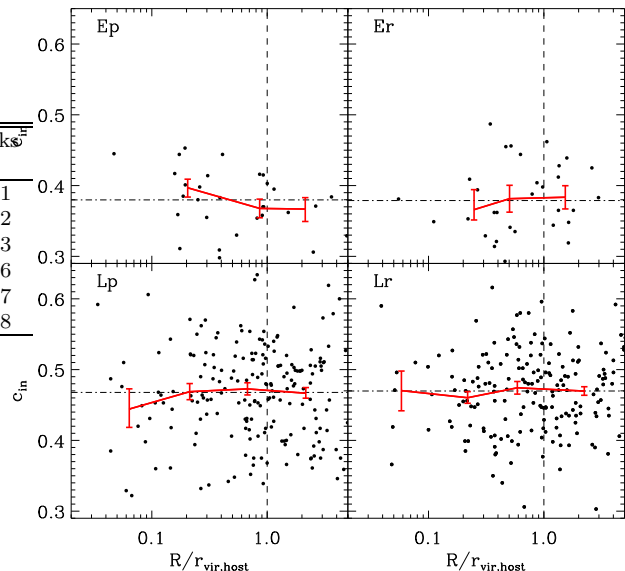


FIG. 14.— Same as Fig. 6, but for concentration index c_{in} .

($R > r_{vir,host}$). For late types, it is seen that the difference in the dispersion of c_{in} between late-type satellites in the prograde and retrograde orbits (see Tab. 1). However, the global median values of c_{in} for two subsamples are similar, and the median values for both subsamples do not show any significant variation with R .

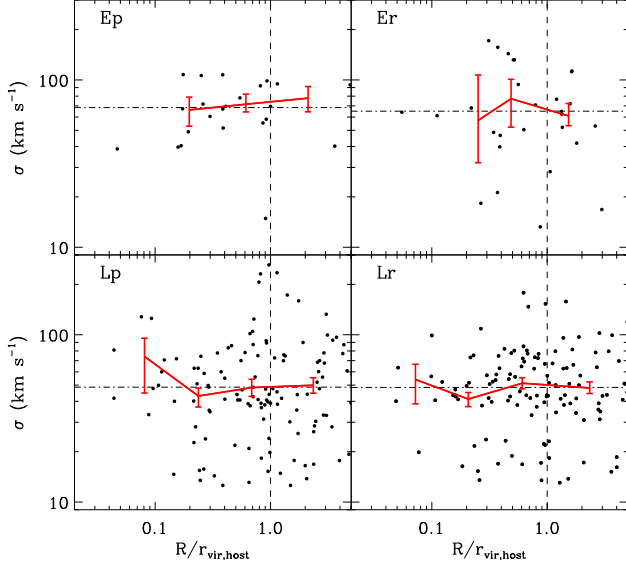
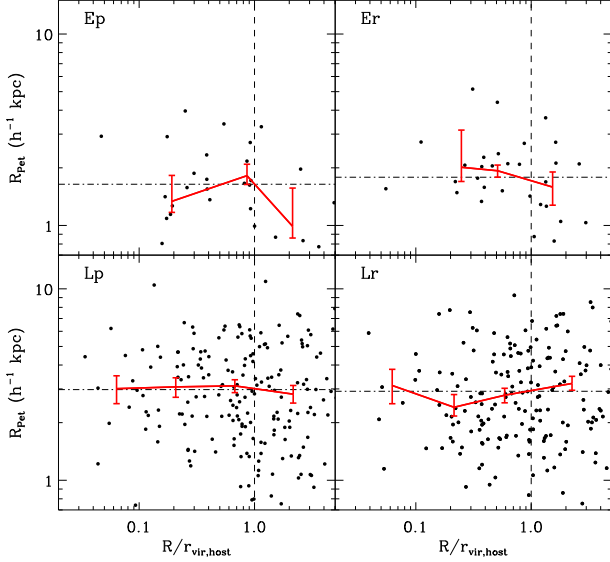
In Figure 15, we plot central velocity dispersions of satellite galaxies. The median values for early types in prograde and retrograde orbits are similar and do not show any significant variation with R . For late types, any significant difference between two subsamples of late-type satellites is not found except for the scatter of σ values.

Figure 16 represents the i -band Petrosian radius R_{Pet} of satellite galaxies. The R_{Pet} for the early-type satellites in the inner region ($R < r_{vir,host}$) appears to be larger than that in the outer region ($R > r_{vir,host}$) (see Tab. 2), while no significant difference between the late-type satellites in prograde and retrograde orbits is not seen.

4. DISCUSSION

4.1. Different Galaxy Samples

We found in Figures 12-13 and Table 1 that the median or its dispersion of W(H α) and $(g-i)$ color gradients can

FIG. 15.— Same as Fig. 6, but for central velocity dispersion σ .FIG. 16.— Same as Fig. 6, but for Petrosian radius R_{Pet} .

be different depending on the orbital motion of late-type satellites. The SFA of early-type satellites in retrograde orbit (Er) also appears to be stronger than those in prograde orbit in the outer region ($r_{\text{vir,host}} < R$) as seen in Figures 11 and 12. Moreover, $(u - r)$ colors of late-type satellites increase as they approach their host galaxies for both satellites in prograde and retrograde orbits, and $(u - r)$ colors of late-type satellites in retrograde orbit in the innermost region ($R < 0.1r_{\text{vir,host}}$) are remarkably large. These differences depending on the orbit can be attributed to the different origin of satellite galaxies, or to the different strength of physical processes that they experience through interactions with host galaxies.

To check whether or not these results are strongly affected by the satellites associated to the host galaxies whose spin direction is determined from the SDSS color images in this study, in Figure 17, we plot $(u - r)$ col-

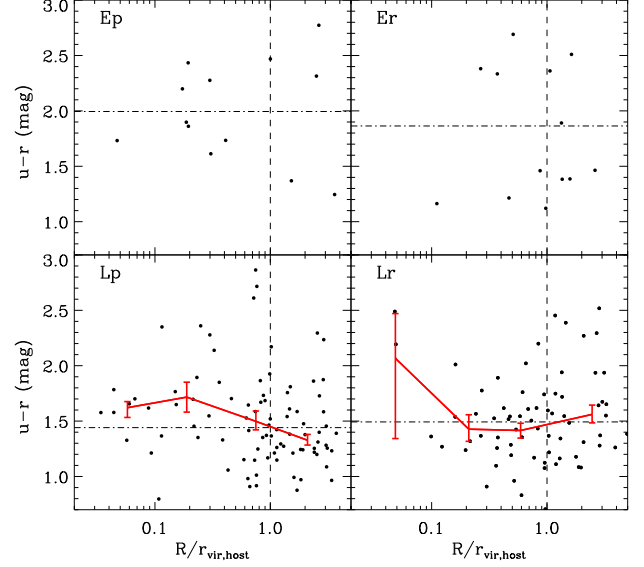


FIG. 17.— Same as Fig. 11, but for the satellites associated to host galaxies whose spin direction is determined from the spectroscopic observations.

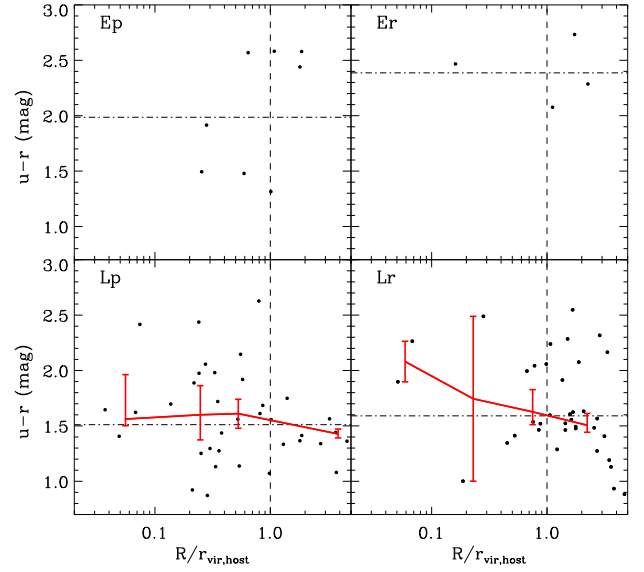


FIG. 18.— Same as Fig. 11, but for the satellites associated to early-type hosts.

ors versus the projected distance to the hosts using the satellites associated to the host galaxies whose spin direction is determined from the spectroscopic observations. For both early and late types, we do not find any significant difference of $(u - r)$ colors between satellites in prograde and retrograde orbits, which is consistent with the result when we use the combined sample of satellites in the host galaxies whose spin direction is determined from the color images or the spectroscopic observations (see Fig. 11). In addition, the late-type satellites in prograde orbits (Lp) show an increase in $(u - r)$ color as decreasing R , which is again similar to the case of late types in prograde orbits using the combined sample of satellites (see Lp in Fig. 11 and Tab. 2). In the result, the results of SFA using the combined sample of satellites are not affected strongly by the satellites associated

to the host galaxies whose spin direction is determined from the color images in this study.

Since the physical parameters of satellite galaxies can be strongly affected by the morphology of host galaxies (e.g., Ann et al. 2008), it is also interesting to compare satellite systems that have early- and late-type host galaxies. To investigate the SFA of satellites around early-type hosts we use a sample of 101 satellites associated with 24 early-type hosts, and show their $(u-r)$ colors in Figure 18. It is seen that $(u-r)$ colors of late-type satellites become redder as R decreases, which was also seen in Figure 11 or 17. For early-type satellites, the small number of satellites prevents us from drawing any firm conclusion.

4.2. Comparison with Other Galaxy Systems

Previously, Park et al. (2008) and Park & Choi (2009) found that galaxy properties strongly depend on the distance and the morphology of the nearest neighbor galaxy. For example, the SFA of galaxies is enhanced as they approach late-type neighbors of comparable luminosity, while it is reduced as they approach early-type neighbors. The structure parameters of galaxies change with the distance to the nearest neighbor galaxy in the same direction independently of neighbor's morphology. Galaxy properties start to change when galaxies approach their nearest neighbor galaxy closer than the virial radius ($r_{\text{vir,nei}}$) of the nearest neighbor galaxy and to change significantly at $R < 0.05r_{\text{vir,nei}}$ where the galaxies in pair start to merge. They interpreted this phenomenon as a result of hydrodynamic interactions within the virial radius of the galaxy plus dark halo system.

The dependence of satellite properties as a function of the distance to the host galaxy in this study can be compared with the case of late-type neighbors in Park & Choi (2009). Since we restrict our analysis to the case of late-type host galaxy, it is expected that the SFA of both early- and late-type satellites increases as they approach the host. However, we found in §3.3 that $(u-r)$ color becomes redder (Fig. 11) and $W(H\alpha)$ hardly changes (Fig. 12) even when late-type satellites approach their late-type hosts. This may be because, unlike the galaxies considered by Park & Choi (2009), the satellites in this study are much fainter and less massive than their hosts. As a result they may not be able to pick up cold gas from their host much, and the enhancement of SFA through interactions with their host is counterbalanced by the quenching by the hot halo gas of the host.

On the other hand, the environment of satellite galaxies can be compared with that of galaxies in galaxy clusters because the member galaxies in a galaxy cluster are bounded within the gravitational potential well of the cluster as the satellites are bounded by their host galaxy. Park & Hwang (2009) studied the dependence of galaxy properties on the clustercentric radius and the environment attributed to the nearest neighbor galaxy using the SDSS galaxies associated with the Abell galaxy clusters. They found that the SFA of late-type galaxies decreases as they approach the cluster center, and suggested that hydrodynamic interactions with nearby early-type galaxies in clusters is the main drive to quenching the SFA of late types. Most cluster galaxies are early types including the brightest cluster galaxies (or cD galaxies), which might be comparable with the case of early-type host

galaxy in the satellite system as seen in Figure 18. The late-type satellites (bottom panels in Fig. 18) become redder as they approach early-type host galaxies, which agrees to the case of galaxy clusters.

Previously, Zinn (1993) pointed out that there are two distinct populations in the halo globular clusters in the Milky Way: old and young halo clusters. Two populations were originally divided by the horizontal branch morphology, but were found to be also separated by their orbital motion in the Milky Way: prograde orbit for old halo clusters and retrograde orbit for young halo clusters (Zinn 1993; van den Bergh 1993; Lee et al. 2007). Therefore, the formation history of old halo clusters with prograde orbit is thought to be different from that of young halo clusters with retrograde orbit (e.g., Eggen et al. 1962 vs. Searle & Zinn 1978). For example, it was suggested that the clusters in retrograde orbit may have been accreted into the Milky Way (e.g., Dinescu et al. 1999), and further that these clusters and Galactic dSphs may have the same origin in accretion or in partially disruption of formerly large parent satellite galaxies (e.g., van den Bergh & Mackey 2004). Therefore, two populations of satellite galaxies with different orbits in this study are also expected to have formed and evolved in different paths, which may be responsible for the different SFA depending on the orbit. The Galactic satellite galaxies also can give us important clues for testing this scenario, but it is not achievable at this moment because of small number (~ 10) of Galactic satellites whose orbital motion is determined.

5. CONCLUSIONS

We have studied the orbital dependence of various galaxy properties in the satellite systems of galaxies in SDSS. Our primary results are summarized as follows.

1. We have found the satellite systems of galaxies at $z < 0.03$, which consist of 8904 satellites associated with 3515 isolated host galaxies.
2. We have determined the spin direction of late-type host galaxies by inspecting the SDSS color images. By combining our results with those from the previous spectroscopic observations in the literature, we obtained 635 satellites associated with 215 host galaxies whose spin directions are known.
3. The number ratio of satellites in prograde orbit to those in retrograde orbit is nearly equal to one, and the peculiar velocity distribution is found to be symmetric. The number ratio of satellites in prograde orbit to those in retrograde orbit (f_{pro}) appears to increase as the projected distance to the host galaxy decreases. However, we do not find any significant difference in the azimuthal distribution of satellites between those in prograde and retrograde orbits.
4. The satellites in retrograde orbit, on average, appear to be slightly brighter than those in prograde orbit. The latter seems to get brighter as they approach late-type hosts, while the former does not show any significant change with the distance to the hosts.

5. For early-type satellites in retrograde orbit, the SFA seems to decrease as they approach host galaxies. For late-type satellites, $(u - r)$ colors of both samples in prograde and retrograde orbits appear to increase as they approach the hosts, while the radial variations of the equivalent width of H α lines for both samples are not significant.
6. The structure parameters of satellites do not seem to be different significantly between galaxies in prograde and retrograde orbits.

The authors are grateful to the anonymous referee for useful comments that improved the original manuscript. CBP acknowledges the support of the National Research Foundation of Korea(NRF) grant funded by the Korea government(MEST) (No. 2009-0062868). Funding for the SDSS and SDSS-II has been provided by the Alfred P. Sloan Foundation, the Participating Institutions, the National Science Foundation, the U.S. Department of Energy, the National Aeronautics and Space Adminis-

tration, the Japanese Monbukagakusho, the Max Planck Society, and the Higher Education Funding Council for England. The SDSS Web Site is <http://www.sdss.org/>. The SDSS is managed by the Astrophysical Research Consortium for the Participating Institutions. The Participating Institutions are the American Museum of Natural History, Astrophysical Institute Potsdam, University of Basel, Cambridge University, Case Western Reserve University, University of Chicago, Drexel University, Fermilab, the Institute for Advanced Study, the Japan Participation Group, Johns Hopkins University, the Joint Institute for Nuclear Astrophysics, the Kavli Institute for Particle Astrophysics and Cosmology, the Korean Scientist Group, the Chinese Academy of Sciences (LAMOST), Los Alamos National Laboratory, the Max-Planck-Institute for Astronomy (MPIA), the Max-Planck-Institute for Astrophysics (MPA), New Mexico State University, Ohio State University, University of Pittsburgh, University of Portsmouth, Princeton University, the United States Naval Observatory, and the University of Washington.

REFERENCES

- Abazajian, K. N., et al. 2009, *ApJS*, 182, 543
 Ann, H. B., Park, C., & Choi, Y.-Y. 2008, *MNRAS*, 389, 86
 Azzaro, M., Zentner, A. R., Prada, F., & Klypin, A. A. 2006, *ApJ*, 645, 228
 Bailin, J., Power, C., Norberg, P., Zaritsky, D., & Gibson, B. K. 2008, *MNRAS*, 390, 1133
 Binney, J., & Tremaine, S. 1987, Princeton, NJ, Princeton University Press, 1987, 747 p.,
 Blanton, M. R., et al. 2003, *AJ*, 125, 2348
 Blanton, M. R., Eisenstein, D., Hogg, D. W., Schlegel, D. J., & Brinkmann, J. 2005, *AJ*, 129, 2562
 Broeils, A. H., & van Woerden, H. 1994, *A&AS*, 107, 129
 Carignan, C., Cote, S., Freeman, K. C., & Quinn, P. J. 1997, *AJ*, 113, 1585
 Chemin, L., et al. 2006, *MNRAS*, 366, 812
 Chen, J., Kravtsov, A. V., Prada, F., Sheldon, E. S., Klypin, A. A., Blanton, M. R., Brinkmann, J., & Thakar, A. R. 2006, *ApJ*, 647, 86
 Chen, J. 2008, *A&A*, 484, 347
 Choi, Y.-Y., Park, C., & Vogele, M. S. 2007, *ApJ*, 658, 884
 Cocato, L., Corsini, E. M., Pizzella, A., Morelli, L., Funes, J. G., & Bertola, F. 2004, *A&A*, 416, 507
 Daigle, O., Carignan, C., Amram, P., Hernandez, O., Chemin, L., Balkowski, C., & Kennicutt, R. 2006, *MNRAS*, 367, 469
 Dinescu, D. I., Girard, T. M., & van Altena, W. F. 1999, *AJ*, 117, 1792
 Eggen, O. J., Lynden-Bell, D., & Sandage, A. R. 1962, *ApJ*, 136, 748
 Epinat, B., et al. 2008a, *MNRAS*, 388, 500
 Epinat, B., Amram, P., & Marcelin, M. 2008b, *MNRAS*, 390, 466
 Falcón-Barroso, J., et al. 2006, *MNRAS*, 369, 529
 Fridman, A. M., Afanasiev, V. L., Dodonov, S. N., Khoruzhii, O. V., Moiseev, A. V., Sil'chenko, O. K., & Zasov, A. V. 2005, *A&A*, 430, 67
 Ganda, K., Falcón-Barroso, J., Peletier, R. F., Cappellari, M., Emsellem, E., McDermid, R. M., de Zeeuw, P. T., & Carollo, C. M. 2006, *MNRAS*, 367, 46
 Garrido, O., Marcelin, M., Amram, P., & Boulesteix, J. 2002, *A&A*, 387, 821
 Garrido, O., Marcelin, M., Amram, P., & Boissin, O. 2003, *A&A*, 399, 51
 Garrido, O., Marcelin, M., & Amram, P. 2004, *MNRAS*, 349, 225
 Garrido, O., Marcelin, M., Amram, P., Balkowski, C., Gach, J. L., & Boulesteix, J. 2005, *MNRAS*, 362, 127
 Han, C., Gould, A., & Sackett, P. D. 1995, *ApJ*, 445, 46
 Héraudeau, P., & Simien, F. 1998, *A&AS*, 133, 317
 Héraudeau, P., Simien, F., Maubon, G., & Prugniel, P. 1999, *A&AS*, 136, 509
 Herbert-Fort, S., Zaritsky, D., Jin Kim, Y., Bailin, J., & Taylor, J. E. 2008, *MNRAS*, 384, 803
 Hernandez, O., Carignan, C., Amram, P., Chemin, L., & Daigle, O. 2005, *MNRAS*, 360, 1201
 Lee, Y.-W., Gim, H. B., & Casetti-Dinescu, D. I. 2007, *ApJ*, 661, L49
 Mihalas, D., & Binney, J. 1981, San Francisco, CA, W. H. Freeman and Co., 1981. 608 p.,
 Noordermeer, E., van der Hulst, J. M., Sancisi, R., Swaters, R. A., & van Albada, T. S. 2005, *A&A*, 442, 137
 Park, C., & Choi, Y.-Y. 2005, *ApJ*, 635, L29
 Park, C., & Choi, Y.-Y. 2009, *ApJ*, 691, 1828
 Park, C., & Hwang, H. S. 2009, *ApJ*, 699, 1595
 Park, C., Gott, J. R., & Choi, Y.-Y. 2008, *ApJ*, 674, 784
 Prada, F., et al. 2003, *ApJ*, 598, 260
 Rhee, M.-H., & van Albada, T. S. 1996, *A&AS*, 115, 407
 Rubin, V. C., Ford, W. K., Jr., Thonnard, N., & Burstein, D. 1982, *ApJ*, 261, 439
 Rubin, V. C., Burstein, D., Ford, W. K., Jr., & Thonnard, N. 1985, *ApJ*, 289, 81
 Rubin, V. C., Waterman, A. H., & Kenney, J. D. P. 1999, *AJ*, 118, 236
 Sales, L., & Lambas, D. G. 2004, *MNRAS*, 348, 1236
 Sales, L., & Lambas, D. G. 2005, *MNRAS*, 356, 1045
 Sales, L. V., Navarro, J. F., Lambas, D. G., White, S. D. M., & Croton, D. J. 2007, *MNRAS*, 382, 1901
 Schlegel, D. J., Finkbeiner, D. P., & Davis, M. 1998, *ApJ*, 500, 525
 Searle, L., & Zinn, R. 1978, *ApJ*, 225, 357
 Sofue, Y. 1997, *PASJ*, 49, 17
 Sofue, Y., Tutui, Y., Honma, M., & Tomita, A. 1997, *AJ*, 114, 2428
 Sofue, Y., Tomita, A., Tutui, Y., Honma, M., & Takeda, Y. 1998, *PASJ*, 50, 427
 Sofue, Y., Koda, J., Nakanishi, H., Onodera, S., Kohno, K., Tomita, A., & Okumura, S. K. 2003, *PASJ*, 55, 17
 Swaters, R. A., Sancisi, R., van Albada, T. S., & van der Hulst, J. M. 2009, *A&A*, 493, 871
 Taylor, C. L., Brinks, E., Grashuis, R. M., & Skillman, E. D. 1995, *ApJS*, 99, 427
 Tegmark, M., et al. 2004, *ApJ*, 606, 702
 Tremonti, C. A., et al. 2004, *ApJ*, 613, 898
 van den Bergh, S. 1993, *ApJ*, 411, 178
 van den Bergh, S., & Mackey, A. D. 2004, *MNRAS*, 354, 713

- van den Bosch, F. C., Yang, X., Mo, H. J., & Norberg, P. 2005, MNRAS, 356, 1233
- Vega Beltrán, J. C., Pizzella, A., Corsini, E. M., Funes, J. G., Zeilinger, W. W., Beckman, J. E., & Bertola, F. 2001, A&A, 374, 394
- Vogt, N. P., Haynes, M. P., Herter, T., & Giovanelli, R. 2004, AJ, 127, 3273
- Wang, Y., Park, C., Yang, X., Choi, Y.-Y., & Chen, X. 2009, ApJ, 703, 951
- Wang, Y., Park, C., Hwang, H. S., & Chen, X. 2010, ApJ, 718, 762
- York, D. G., et al. 2000, AJ, 120, 1579
- Zaritsky, D., Smith, R., Frenk, C., & White, S. D. M. 1993, ApJ, 405, 464
- Zaritsky, D., Smith, R., Frenk, C., & White, S. D. M. 1997, ApJ, 478, 39
- Zinn, R. 1993, The Globular Cluster-Galaxy Connection, 48, 38